

# Space-Variant Channelized Preconditioner Design for 3D Iterative CT Reconstruction

Lin Fu, Zhou Yu, Jean-Baptiste Thibault, Bruno De Man, Madison G. McGaffin, and Jeffrey A. Fessler

**Abstract—** Preconditioners, especially diagonal ones, have been key ingredients in several state-of-the-art optimization algorithms for transmission and emission tomographic image reconstruction. But it remains challenging to design robust, non-diagonal preconditioners that can account for various space-variant factors such as fan-beam/helical sampling geometry, non-uniform statistical weights, and object-dependent regularization. In this study, we propose a channelized preconditioner design that decomposes a preconditioner into multiple channels that represent different frequency sub-bands and/or orientations. Each channel is associated with a spatial weighting map to modulate its gain at different spatial locations. The multi-channel design has the potential to provide more degrees of freedom in controlling the localized spectral response of the preconditioner without incurring excessive computational overhead. Initial application to maximum *a posteriori* probability image reconstruction from helical x-ray CT data is presented here.

**Index Terms—** computed tomography, iterative image reconstruction, preconditioner.

## I. INTRODUCTION

Model-based iterative reconstruction (MBIR) techniques for x-ray computed tomography (CT) have been developed over a decade ago [1], [2], but have only been recently introduced commercially on multi-slice clinical CT scanners. Based on the principles of maximum *a posteriori* probability (MAP) estimation, the model-based approach improves multiple aspects of image quality, and has demonstrated potential dose savings in recent clinical trials compared to the conventional filtered backprojection (FBP) method and other state-of-the-art CT reconstruction methods [3], [4].

Due to the complexity of various geometrical, physical, and statistical models being employed by MBIR, and the large size of data acquired by today's multi-slice CT scanners, the computational cost of MBIR remains a major impediment to its widespread use in clinical environments. It is a topic of growing interest to develop accelerated MBIR algorithms. This study will focus on gradient-based simultaneous-update optimization algorithms, which have relatively high level of parallelism and could potentially take full advantage of many-core computing devices.

The project described was supported by Grant Number 1-R01-HL-098686 from NIH and its contents are solely the responsibility of the authors and do not necessarily represent the official views of the NIH.

L. Fu and B. De Man are with GE Global Research Center, Niskayuna NY 12309. Z. Yu and J.-B. Thibault are with GE Healthcare Technologies, Waukesha, WI 53188. M. G. McGaffin and J. A. Fessler are with the Electrical Engineering and Computer Science department, University of Michigan, Ann Arbor, MI 48109.

Standard gradient-based iterations usually converge slowly for large-scale ill-conditioned problems. Effective preconditioning techniques are essential for their acceleration and practical success. Various forms of preconditioners have been studied in the context of iterative tomographic reconstruction. Diagonal scaling matrix is the simplest form of preconditioner. Several widely used iterative algorithms in emission and transmission reconstruction can be viewed as diagonally-preconditioned gradient descent algorithms (for instance EM [5], [6], SQS [7], and ML-TR [8]). Diagonal preconditioners are also commonly combined with other optimization algorithms such as conjugate-gradient to achieve more significant acceleration [9–11]. Despite their effectiveness and robustness, diagonal preconditioners are considered relatively conservative approximations to the inverse of the Hessian matrix and can only provide suboptimal acceleration.

Non-diagonal, Fourier preconditioners have the potential to address the off-diagonal structure of the Hessian. Such preconditioners are also attractive because of their close connection to the ramp-filter used in FBP reconstruction. These preconditioners can bring dramatic acceleration for space-invariant problems [12], but they are less effective for space-variant reconstruction due to factors such as irregular geometric sampling, non-uniform statistical noise modeling, and location-dependent image priors.

To improve convergence rates in space-variant reconstruction, Booth and Fessler proposed a preconditioning technique based on the product of a Fourier kernel and a particular diagonal matrix [11]. Such combined preconditioner yields significantly faster convergence than either Fourier or diagonal preconditioning alone. In a subsequent work, the Fourier component was further generalized by interpolation among multiple FFTs to provide more effective handling of space-variant regularization strength [13]. More recently, operator splitting methods has been proposed for preconditioners to better address shift-variant problems [14], [15].

Some promising results have recently been reported in applying preconditioning techniques to accelerating CT MBIR [16]. It will be of great interest to develop more effective and efficient preconditioners for multi-slice medical CT systems where the geometric sampling can be incomplete or truncated, and the statistical noise is highly anisotropic. To properly account for the space-variant effects, we would need a sufficient degree of freedom in controlling the local frequency response of the preconditioner without incurring excessive computational overhead. In this study, we propose a channelized preconditioner design, in which the preconditioner is decomposed into different channels representing different frequency sub-bands and/or orientations. A spatial

weighting map is applied to each channel to modulate its gain at different locations. While single channel may be restrictive in modeling space-variant frequency response, the combination of multiple channels may provide a sufficient degree of freedom in controlling the local frequency response without incurring excessive computation overhead.

## II. THEORY

### A. MAP cost function

One approach to statistical image reconstruction in x-ray CT uses a MAP cost function in the form of

$$\Phi(\mathbf{x}) = -L(\mathbf{Ax}; \mathbf{y}) + U(\mathbf{x}),$$

where  $\mathbf{x} = \{x_1, \dots, x_N\}$  denotes the vector of unknown 3D image space;  $\mathbf{y} = \{y_1, \dots, y_M\}$  is the vector of sinogram measurements;  $\mathbf{A} \in \mathbb{R}^{M \times N}$  denotes the system matrix;  $-L(\cdot, \cdot)$  is the negative log likelihood term that penalizes the inconsistency between the estimated projection data and the physical measurements;  $U(\mathbf{x})$  is the regularization function that penalizes the noise in the image.

In this study, we use Gaussian log likelihood function with the noise covariance matrix  $\mathbf{W}^{-1}$  and  $L(\mathbf{Ax}, \mathbf{y}) = -\frac{1}{2}(\mathbf{y} - \mathbf{Ax})^T \mathbf{W}(\mathbf{y} - \mathbf{Ax})$ . The regularization function  $U(\mathbf{x})$  is expressed by a Markov Random Field (MRF) in the form of  $U(\mathbf{x}) = \sum_{k \in \mathcal{N}_j, k > j} \omega_{jk} \rho(x_j - x_k)$ , with  $\mathcal{N}_j$  denoting the collection of the neighboring pixels for location  $j$ ,  $\omega_{jk}$  representing the penalty strength between pixel  $j$  and  $k$ , and  $\rho(\cdot)$  being a prior potential function. We use the  $q$ -GGMRF prior with  $\rho(\Delta) = \frac{|\Delta|^p}{1 + \frac{|\Delta|^p}{c}}$  and  $1 \leq q \leq p \leq 2$  to ensure convexity [2].

### B. Hessian matrix and local spectral analysis

The Hessian matrix for the MAP cost function is

$$\mathbf{H}(\mathbf{x}) \triangleq \nabla^2 \Phi(\mathbf{x}) = \mathbf{A}^T \mathbf{W} \mathbf{A} + \nabla^2 U(\mathbf{x}).$$

We would like the preconditioner  $\mathbf{M}$  to be an effective approximation to the inverse of the Hessian matrix, so that  $\mathbf{MH} \approx \mathbf{I}$ , or the condition number of  $\mathbf{MH}$  be minimized. This direct matrix optimization problem seems not tractable so approximations have to be used.

Based on the concept of local shift invariance [17], [18], it is generally assumed that the Hessian matrix is locally block-Toeplitz, so that it can be approximately diagonalized by Fourier transforms. The local spectral representation of  $\mathbf{H}(\mathbf{x})$  at the location of the  $j$ th pixel is

$$\begin{aligned} \mathbf{h}^j(\mathbf{x}) &\triangleq \mathbf{H}(\mathbf{x}) \mathbf{e}^j \\ &= \mathbf{Q}^T \text{diag}\{\boldsymbol{\lambda}^j + \boldsymbol{\mu}^j(\mathbf{x})\} \mathbf{Q} \mathbf{e}^j, \end{aligned}$$

where  $\mathbf{h}^j(\mathbf{x})$  is the  $j$ th column of  $\mathbf{H}(\mathbf{x})$ ;  $\mathbf{e}^j$  is the  $j$ th unit vector;  $\mathbf{Q}$  represents a discrete Fourier transform;  $\boldsymbol{\lambda}^j$  and  $\boldsymbol{\mu}^j$  are the Fourier transforms of the  $j$ th column of  $\mathbf{A}^T \mathbf{W} \mathbf{A}$  and  $\nabla^2 U(\mathbf{x})$ , respectively.

$$\begin{aligned} \boldsymbol{\lambda}^j &= \text{diag}\{\mathbf{Q} \mathbf{e}^j\}^{-1} \mathbf{Q} [\mathbf{A}^T \mathbf{W} \mathbf{A} \mathbf{e}^j], \\ \boldsymbol{\mu}^j(\mathbf{x}) &= \text{diag}\{\mathbf{Q} \mathbf{e}^j\}^{-1} \mathbf{Q} [\nabla^2 U(\mathbf{x}) \mathbf{e}^j]. \end{aligned}$$

The term  $\text{diag}\{\mathbf{Q} \mathbf{e}^j\}^{-1}$  adds the appropriate complex exponentials.

### C. Ramp-filter based preconditioner

In a previous study [16], we designed a ramp-filter based preconditioner based on the combined diagonal/circulant formulation proposed by Fessler and Booth [13]. In this study, we implement a similar but improved design, and will compare its performance to the channelized preconditioner to be introduced in the next few sections. The ramp-based preconditioner in this study takes the form of

$$\mathbf{M}_{\text{ramp}} = \text{diag}(\Lambda_j)^{-1} \mathbf{K} \text{diag}(\Lambda_j)^{-1},$$

where  $\mathbf{K}$  is a space-invariant isotropic Fourier kernel, and  $\Lambda_j$  is a particular spatial weighting factor that makes the preconditioner space-variant [13]. The filter kernel  $\mathbf{K}$  is designed based on a continuous-space approximation to the matrix spectra  $\boldsymbol{\lambda}^j$  and  $\boldsymbol{\mu}^j$  [19]. The frequency response of the filter resembles an apodized ramp-filter

$$K(e^{j2\pi f}) = \left\{ \frac{1}{|f| + \delta_0} + \left( \frac{\kappa_0}{\Lambda_0} \right)^2 2\sin^2(\pi f) \right\}^{-1},$$

where  $-0.5 < f < 0.5$  is normalized digital frequency, and  $\Lambda_0$ ,  $\delta_0$ , and  $\kappa_0$  are parameters to adjust the shape of the frequency response. The filter kernel can be adjusted to match the Hessian only at a single location, thus it is restrictive in modeling highly space-variant system response.

### D. Channelized preconditioner

To provide more degrees of freedom in approximating the space-variant factors in the Hessian, we propose a channelized preconditioner design, in which the preconditioner consists of  $K$  predetermined frequency channels:

$$\mathbf{M}(\mathbf{x}) = \sum_{k=1}^K \text{diag}\{\mathbf{t}_k(\mathbf{x})\} \mathbf{M}_k \text{diag}\{\mathbf{t}_k(\mathbf{x})\},$$

where each channel represents a frequency sub-band and/or spatial orientation.  $\mathbf{M}_k$  is a positive-definite filter that defines the frequency response of the  $k$ th channel, and  $\mathbf{t}_k$  is a spatial weighting map that modulates the gain of the  $k$ th channel at different locations. By splitting the preconditioner into different channels, we could control the gain of each channel independently, which gives the potential to incorporate more space-variant effects. The ramp-based preconditioner introduced earlier can be viewed as a special case where a single high-pass channel is used.

### E. Channel design

To design the channelized preconditioner, we first determine the number of channels and the frequency response of each channel. The channels are like basis functions. More channels will improve the frequency resolution but also increase design complexity and computational overhead. In this initial study, making no attempt to optimize the channel

design in general, we explore the possibility of using only three channels ( $K = 3$ ). These channels could be implemented in either frequency domain or space domain. Here we propose image-space kernels with very small footprint ( $3 \times 3$ ), which has less computational overhead than implementing these kernels in Fourier space.

$$\begin{aligned} \text{Ker}\mathbf{M}_1 &= \left\{ \begin{bmatrix} 0 & 0 & 0 \\ 0 & 0 & 0 \\ 0 & 0 & 0 \end{bmatrix}, \begin{bmatrix} 1 & 2 & 1 \\ 2 & 12 & 2 \\ 1 & 2 & 1 \end{bmatrix}, \begin{bmatrix} 0 & 0 & 0 \\ 0 & 0 & 0 \\ 0 & 0 & 0 \end{bmatrix} \right\} \\ \text{Ker}\mathbf{M}_2 &= \left\{ \begin{bmatrix} -1 & -2 & -1 \\ -2 & 12 & -2 \\ -1 & -2 & -1 \end{bmatrix}, \begin{bmatrix} -2 & -4 & -2 \\ -4 & 24 & -4 \\ -2 & -4 & -2 \end{bmatrix}, \begin{bmatrix} -1 & -2 & -1 \\ -2 & 12 & -2 \\ -1 & -2 & -1 \end{bmatrix} \right\} \\ \text{Ker}\mathbf{M}_3 &= \left\{ \begin{bmatrix} 1 & 2 & 1 \\ 2 & -12 & 2 \\ 1 & 2 & 1 \end{bmatrix}, \begin{bmatrix} -2 & -4 & -2 \\ -4 & 24 & -4 \\ -2 & -4 & -2 \end{bmatrix}, \begin{bmatrix} 1 & 2 & 1 \\ 2 & -12 & 2 \\ 1 & 2 & 1 \end{bmatrix} \right\} \end{aligned}$$

The first channel represents low frequency in plane (x-y). The second one represents high frequency in plane (x-y) and low frequency across plane (z). And the third one represents high frequency both in plane (x-y) and across planes (z). These channels are approximately isotropic, i.e., no angular preference. However it is possible to design channels with different spatial orientations to account for anisotropic effects in the Hessian. This will be a potential topic for further investigation. As will be shown in the initial results here, even the relatively simple three-channel design can provide significant improvement over the conventional diagonal or combined diagonal/circulant preconditioners.

#### F. Spatial weighting design

Now we will design the spatial weighting  $\mathbf{t}_k$  associated with each channel. We would like to design  $\mathbf{t}_k$  so that

$$\mathbf{M}(\mathbf{x})\mathbf{H}(\mathbf{x}) \approx \mathbf{I}.$$

In local spectral representation, this condition becomes

$$\left[ \mathbf{Q}^T \left( \sum_{k=1}^K t_{kj}^2 \text{diag}\{\mathbf{v}_k\} \right) \mathbf{Q} \right] \left[ \mathbf{Q}^T \text{diag}\{\lambda^j + \mu^j(\mathbf{x})\} \mathbf{Q} \right] \approx \mathbf{I},$$

where  $\mathbf{v}_k$  denote the Fourier transform of  $\mathbf{M}_k$ , i.e.,  $\mathbf{M}_k = \mathbf{Q}^T \text{diag}\{\mathbf{v}_k\} \mathbf{Q}$ , and  $t_{kj}$  is the  $j$ th element of the  $\mathbf{t}_k$ , representing the spatial weighting for the  $k$ th channel at location  $j$ . After simplification, we obtain a system of linear equations that  $\mathbf{t}_k$  should satisfy:

$$\sum_{k=1}^K \mathbf{v}_k \odot (\lambda^j + \mu^j(\mathbf{x})) t_{kj}^2 \approx \mathbf{1},$$

where “ $\odot$ ” denote element-wise multiplication. This condition means we would like the preconditioned problem to have a “flat” spectrum. The equation is over-determined and does not have a strict solution. Although various generalized inverse or optimization based methods may be used to solve such an over-determined problem, here we propose to find an approximate solution that only satisfies the equations at  $K$  frequency samples,  $\mathbf{f}_1 \dots \mathbf{f}_K$ . In matrix form this yields

$$\begin{bmatrix} v_{11} & \dots & v_{1K} \\ \vdots & \ddots & \vdots \\ v_{K1} & \dots & v_{KK} \end{bmatrix} \begin{bmatrix} (\lambda_1^j + \mu_1^j) t_{1j}^2 \\ \vdots \\ (\lambda_K^j + \mu_K^j) t_{Kj}^2 \end{bmatrix} = \begin{bmatrix} 1 \\ \vdots \\ 1 \end{bmatrix}$$

where  $v_{ik} \triangleq v_i(\mathbf{f}_k)$ ,  $\lambda_k^j \triangleq \lambda^j(\mathbf{f}_k)$ ,  $\mu_k^j \triangleq \mu^j(\mathbf{f}_k, \mathbf{x})$ . Assuming the frequency channels are linearly independent, the solution is obtained by inverting the  $K$ -by- $K$  matrix formed by  $\{v_{ik}\}$

$$\begin{bmatrix} t_{1j}^2 \\ \vdots \\ t_{Kj}^2 \end{bmatrix} = \begin{bmatrix} \lambda_1^j + \mu_1^j & & \\ & \ddots & \\ & & \lambda_K^j + \mu_K^j \end{bmatrix}^{-1} \begin{bmatrix} v_{11} & \dots & v_{1K} \\ \vdots & \ddots & \vdots \\ v_{K1} & \dots & v_{KK} \end{bmatrix}^{-1} \begin{bmatrix} 1 \\ \vdots \\ 1 \end{bmatrix}.$$

If the channels have good frequency separation, we may further assume the  $K$ -by- $K$  matrix is approximately diagonal, which yields a simple approximate solution:

$$t_{jk}^2 = \frac{1}{(\lambda_k^j + \mu_k^j) v_{kk}}.$$

Computing  $\mathbf{t}_k$ s using the above expression still requires  $\lambda_k^j + \mu_k^j$  be obtained first. Efficient methods to compute  $\lambda_k^j$  have been proposed, where computation may be performed only at sparsely sampled locations and then be interpolated to others [20][21].  $\lambda_k^j$  and  $\mu_k^j$  may also be obtained using continuous-space approximations.

The spectral coefficients  $\lambda^j$  are not only space-variant but also anisotropic due to the high dynamic range of the statistical weights  $\mathbf{W}$ . Since we are only using approximately isotropic channels in this initial study, we design the preconditioner by matching the frequency response in the angular direction associated with the strongest statistical weights. This is a more conservative choice compared with matching the averaged frequency response over all angular directions, and helps make the preconditioner more robust. We may also apply empirical adjustment to gain of the spatial-frequency channels. For example, we may reduce the gain of high frequency channels in the regions where the sampling is incomplete and the Hessian is highly space-variant.

### III. APPLICATION TO HELICAL CT DATA

We tested the algorithms using a chest scan acquired on a 64-slice GE HD750 CT scanner at 120 kV with a helical pitch of one. The reconstruction field-of-view was 70 cm in diameter and 8.5 cm in Z direction, with image matrix size of  $600 \times 600 \times 136$ . We compared the convergence rates of four numerical algorithms: standard conjugate-gradient (CG), CG with separable quadratic surrogate (SQS) preconditioner [7], CG with ramp-based preconditioner, and CG with the proposed 3-channel preconditioner. All algorithms are initialized with standard FBP reconstructions and run with 10 iterations. An approximately fully converged reference reconstruction is generated by 20 iterations of non-homogenous iterative coordinate descent (ICD) [2], [22].

Sample images reconstructed from different methods are shown in Figure 1. At only 10 iterations, the proposed channelized preconditioner generates images that have similar visual quality as the reference MBIR solution, while other reconstruction methods show less satisfactory image

quality. Figure 2 shows the image-domain L2 distance to the reference solution as a function of iteration number. The channelized preconditioner clearly achieves the fastest convergence rate.



Figure 1. Sample reconstructions with different methods. All reconstructions are initialized with the FBP image. Display window = [-200 200] HU.

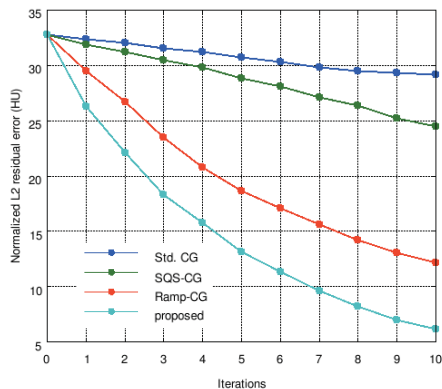


Figure 2. Convergence curves.

#### IV. SUMMARY AND DISCUSSION

We have presented a channelized preconditioner design for CT MBIR problems. In the proposed design, the channels represent different spatial frequency sub-bands, and the gain for each channel is space-variant and independently modulated by a spatial weighting map. The introduction of the multiple channels has the potential to provide more degrees of freedom in approximating space-variant factors in the Hessian matrix. Compared to the channelized design, the conventional diagonal preconditioners can be viewed as a single all-pass channel, while the ramp-based preconditioner can be viewed as a single high-pass channel, both being special cases of the proposed channelized design.

Unlike previous methods based on FFTs which aim to model the frequency response accurately, we recognize the tradeoff among frequency resolution, space-variance, and

computational cost, and used very small  $3 \times 3 \times 3$  preconditioner kernels which bring little computational overhead to MBIR. The new algorithm is tested with helical CT data and effective acceleration compared to other conventional types of diagonal and Fourier preconditioners is illustrated.

#### V. REFERENCES

- [1] B. De Man and J. A. Fessler, "Statistical iterative reconstruction for X-ray computed tomography," in *Biomedical Mathematics*, G. Wang, Y. Censor, and J. Ming, Eds. Springer, 2009.
- [2] J.-B. Thibault, K. D. Sauer, C. A. Bouman, and J. Hsieh, "A three-dimensional statistical approach to improved image quality for multislice helical CT," *Med. Phys.*, vol. 34, no. 11, pp. 4526–4544, 2007.
- [3] P. J. Pickhardt, M. G. Lubner, D. H. Kim, J. Tang, J. A. Ruma, A. M. del Rio, and G.-H. Chen, "Abdominal CT with model-based iterative reconstruction (MBIR): initial results of a prospective Trial comparing ultralow-dose with standard-dose imaging," *American Journal of Roentgenology*, vol. 199, p. to appear, 2012.
- [4] A. Neroladaki, D. Botsikas, S. Boudabbous, C. D. Becker, and X. Montet, "Computed tomography of the chest with model-based iterative reconstruction using a radiation exposure similar to chest X-ray examination: preliminary observations," *European Radiology*, p. ahead of print, available online, 2012.
- [5] K. Lange and R. Carson, "EM reconstruction algorithms for emission and transmission tomography," *J. Comp. Assisted Tomo.*, vol. 8, pp. 306–316, 1984.
- [6] L. Kaufman, "Implementing and accelerating the em algorithm for positron emission tomography," *IEEE Transactions on Medical Imaging*, vol. 6, no. 1, pp. 37–51, 1987.
- [7] H. Erdogan and J. A. Fessler, "Ordered subsets algorithms for transmission tomography," *Phys. Med. Biol.*, vol. 44, pp. 2835–51, 1999.
- [8] B. De Man, J. Nuyts, P. Dupont, G. Marchal, and P. Suetens, "An iterative maximum-likelihood polychromatic algorithm for CT," *IEEE Transactions on Medical Imaging*, vol. 20, no. 10, pp. 999–1008, 2001.
- [9] E. U. Mumcuoglu, R. Leahy, S. R. Cherry, and Z. Zhou, "Fast gradient-based methods for Bayesian reconstruction of transmission and emission PET images," *IEEE Trans. Med. Imag.*, vol. 13, pp. 687–701, 1994.
- [10] J. Qi, R. M. Leahy, S. R. Cherry, A. Chatziioannou, and T. H. Farquhar, "High resolution 3D Bayesian image reconstruction using the microPET small animal scanner," *Phys. Med. Biol.*, vol. 43, pp. 1001–13, 1998.
- [11] S. D. Booth and J. A. Fessler, *Combined diagonal/Fourier preconditioning methods for image reconstruction in emission tomography*, vol. 2. 1995, pp. 441–444.
- [12] N. H. Clinthorne, T. S. Pan, P. C. Chiao, W. L. Rogers, and J. A. Stamos, "Preconditioning methods for improved convergence rates in iterative reconstructions," *IEEE Trans. Med. Imag.*, vol. 12, no. 1, pp. 78–83, 1993.
- [13] J. A. Fessler and S. D. Booth, "Conjugate-gradient preconditioning methods for shift-variant PET image reconstruction," *IEEE Trans. Imag. Proc.*, vol. 8, no. 5, pp. 688–99, 1999.
- [14] S. Ramani and J. A. Fessler, "A splitting-based iterative algorithm for accelerated statistical x-ray CT reconstruction," *IEEE Trans. Med. Imag.*, vol. 31, no. 3, pp. 677–88, 2012.
- [15] M. G. McGaffin, S. Ramani, and J. A. Fessler, "Reduced memory augmented Lagrangian algorithm for 3D iterative x-ray CT image reconstruction," in *Proc. SPIE 8313*, 2012, p. 831327.
- [16] L. Fu, B. De Man, K. Zeng, T. M. Benson, Z. Yu, G. Cao, and J.-B. Thibault, "A Preliminary Investigation of 3D Preconditioned Conjugate Gradient Reconstruction for Cone-Beam CT," in *Proc. SPIE 8313*, 2012, p. 831330.
- [17] J. A. Fessler and W. L. Rogers, "Spatial resolution properties of penalized-likelihood image reconstruction methods: Space-invariant tomographs," *IEEE Trans. Imag. Proc.*, vol. 5, pp. 1346–1358, 1996.
- [18] J. Qi and R. M. Leahy, "Resolution and noise properties of MAP reconstruction for fully 3-D PET," *IEEE Trans. Med. Imag.*, vol. 19, no. 5, pp. 493–506, 2000.
- [19] J. A. Fessler, "Analytical approach to regularization design for isotropic spatial resolution," in *IEEE Nuc. Sci. Symp. Med. Im. Conf.*, 2003, pp. 2022–6.
- [20] J. W. Stayman and J. A. Fessler, "Compensation for nonuniform resolution using penalized-likelihood reconstruction in space-variant imaging systems," *IEEE Trans. Med. Imag.*, vol. 23, no. 3, pp. 269–284, 2004.
- [21] L. Yang, J. Zhou, and J. Qi, "Penalized maximum-likelihood image reconstruction for 3D breast lesion detection," in *IEEE Nuclear Science Symposium Conference*, 2012.
- [22] Z. Yu, J.-B. Thibault, C. A. Bouman, K. D. Sauer, and J. Hsieh, "Fast model-based X-ray CT reconstruction using spatially nonhomogeneous ICD optimization," *IEEE Trans. Imag. Proc.*, vol. 20, no. 1, pp. 161–175, 2011.